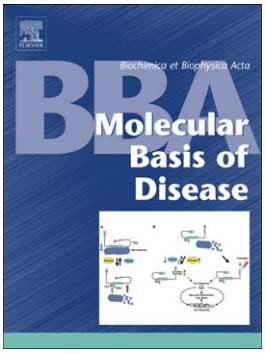

Elevated glutaric acid levels in Dhtkd1 -/Gcdh- double knockout mice challenge our current understanding of lysine metabolism

Caroline Biagosch, RagaDeepthi Ediga, Svenja-Viola Hensler, Michael Faerberboeck, Ralf Kuehn, Wolfgang Wurst, Thomas Meitinger, Stefan Kölker, Sven Sauer, Holger Prokisch

PII: S0925-4439(17)30155-2
DOI: doi:10.1016/j.bbadis.2017.05.018
Reference: BBADIS 64774

To appear in: *BBA - Molecular Basis of Disease*

Received date: 3 February 2017
Revised date: 28 April 2017
Accepted date: 17 May 2017

Please cite this article as: Caroline Biagosch, RagaDeepthi Ediga, Svenja-Viola Hensler, Michael Faerberboeck, Ralf Kuehn, Wolfgang Wurst, Thomas Meitinger, Stefan Kölker, Sven Sauer, Holger Prokisch, Elevated glutaric acid levels in Dhtkd1 -/Gcdh- double knockout mice challenge our current understanding of lysine metabolism, *BBA - Molecular Basis of Disease* (2017), doi:10.1016/j.bbadis.2017.05.018

Elevated glutaric acid levels in Dhtkd1-/Gcdh- double knockout mice challenge our current understanding of lysine metabolism

Caroline Biagosch [*1,2], RagaDeepthi Ediga [*,3], Svenja-Viola Hensler [1,2,4], Michael Faerberboeck [2], Ralf Kuehn [4], Wolfgang Wurst [4], Thomas Meitinger[1,2], Stefan Kölker[3], Sven Sauer[*,3], Holger Prokisch[*1,2]

[1] Institute of Human Genetics, Technical University Munich, Trogerstr. 32, 81675 Munich, Germany;
[2] Institute of Human Genetics, Helmholtz Zentrum Munich, Ingolstädter Landstr. 1, 85764 Neuherberg, Germany;
[3] University Hospital Heidelberg, Centre for Child and Adolescent Medicine, Division of Neuropediatrics and Metabolic Medicine, Im Neuenheimer Feld 430, D-69120 Heidelberg, Germany
[4] Institute of Developmental Genetics, Helmholtz Zentrum München, Ingolstädter Landstr. 1, 85764 Neuherberg, Germany

*These authors contributed equally to this study.

Correspondence to PD Dr. rer. nat. Sven Sauer; Sven.Sauer@med.uni-heidelberg.de, Dr. rer. nat. Holger Prokisch; prokisch@helmholtz-muenchen.de

Keywords

Glutaric Aciduria Type I, 2-aminoadipic 2-oxoadipic aciduria, L-Lysine, GCDH, DHTKD1, glutaric acid

Highlights

- **Generation of *Dhtkd1*$^{-/-}$ mice as a model of 2-aminoadipic/ 2-oxoadipic aciduria**
- ***Dhtkd1*$^{-/-}$ mice reproduce the biochemical phenotype of patients**
- **Generation of *Dhtkd1*$^{-/-}$/*Gcdh*$^{-/-}$ mice as treatment model for glutaric aciduria type 1**
- ***Dhtkd1* knockout does not rescue lysine toxicity in Gcdh deficient mice**
- **Modified concept of mammalian L-lysine degradation**

Abstract

Glutaric aciduria type I (GA-I) is a rare organic aciduria caused by the autosomal recessive inherited deficiency of glutaryl-CoA dehydrogenase (GCDH). GCDH deficiency leads to disruption of L-lysine degradation with characteristic accumulation of glutarylcarnitine and neurotoxic glutaric acid (GA), glutaryl-CoA, 3-hydroxyglutaric acid (3-OHGA). DHTKD1 acts upstream of GCDH, and its deficiency leads to none or often mild clinical phenotype in humans, 2-aminoadipic 2-oxoadipic aciduria. We hypothesized that inhibition of DHTKD1 may prevent the accumulation of neurotoxic dicarboxylic metabolites suggesting DHTKD1 inhibition as a possible treatment strategy for GA-I. In order to validate this hypothesis we took advantage of an existing GA-I (*Gcdh*$^{-/-}$) mouse model and established a Dhtkd1 deficient mouse model. Both models reproduced the biochemical and clinical phenotype observed in patients. Under challenging conditions of a high lysine diet, only *Gcdh*$^{-/-}$ mice but not *Dhtkd1*$^{-/-}$ mice developed clinical symptoms such as lethargic behaviour and weight loss. However, the genetic Dhtkd1 inhibition in *Dhtkd1*$^{-/-}$*/Gcdh*$^{-/-}$ mice could not rescue the GA-I phenotype. Biochemical results confirm this finding with double knockout mice showing similar metabolite accumulations as *Gcdh*$^{-/-}$ mice with high GA in brain and liver. This suggests that DHTKD1 inhibition alone is not sufficient to treat GA-I, but instead a more complex strategy is needed. Our data highlights the many unresolved questions within the L-lysine degradation pathway and provides evidence for a so far unknown mechanism leading to glutaryl-CoA.

Graphical abstract

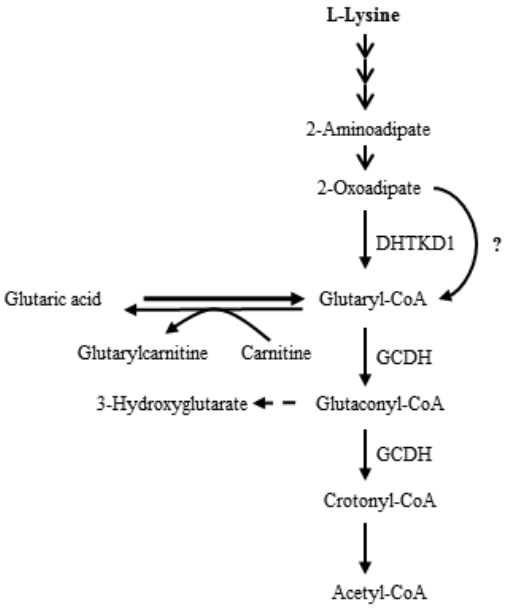

1. Introduction

Glutaric aciduria type I (GA-I; MIM # 231670) is an autosomal recessive metabolic disorder of the final degradative pathway of L-lysine, L-hydroxylysine and L-tryptophan caused by deficiency of glutaryl-CoA dehydrogenase (GCDH; EC 1.3.99.7). The estimated prevalence of GA-I is about 1:110,000 newborns [1] with a significantly higher frequency in known high risk populations [2] [3] [4] [5] [6]. GCDH deficiency leads to an accumulation of the toxic metabolites glutaryl-CoA, glutaric acid (GA) and 3-hydroxyglutaric acid (3-OH-GA) as well as of non-toxic glutarylcarnitine (C5DC). Characteristically, untreated patients develop acute or insidious onset striatal damage and, subsequently, a complex movement disorder with predominant dystonia, most commonly between age 3 and 36 months [5] [7].

The neuropathogenesis of GA-I is attributed to (1) overstimulation of glutamatergic neurotransmission by 3-OH-GA [8] [9]; (2) inhibition of 2-oxoglutarate dehydrogenase complex in the tricarboxylic acid cycle by glutaryl-CoA [10]; (3) inhibition of the astrocyte-neuron dicarboxylic shuttle by GA and - less pronounced - by 3-OH-GA [11]; and (4) disturbance of cerebral hemodynamics resulting in expanded cerebrospinal fluid volume [12]. The prerequisite of these neurotoxic mechanism is that the toxic metabolites are *de novo* synthesized and, subsequently, trapped in the brain compartment due to very limited efflux across the blood-brain barrier [13] [14] [15].

Gcdh knockout mice (*Gcdh*$^{-/-}$) have a complete loss of Gcdh and biochemically resemble GA-I patients but do not spontaneously develop a clinical phenotype, and striatal damage cannot be triggered by catabolic stress [16] [17]. A neurological phenotype can be induced by feeding high lysine diet resulting in massive cerebral accumulation of toxic metabolites and death [18]. The severity of the induced biochemical and clinical phenotype is modulated by gender, genetic background, and daily oral lysine supply [19].

In patients, striatal damage can be prevented if affected individuals are diagnosed before the onset of irreversible neurologic symptoms and treated by low lysine diet, carnitine supplementation and, on demand, emergency treatment (during episodes that are likely to induce catabolism) [1] [20].

In analogy, the same therapeutic means have been shown to reduce cerebral toxin accumulation and prevent systemic carnitine depletion in *Gcdh*$^{-/-}$ mice [17] [18].

Even though this metabolic treatment is thought to be safe [21] and effective [1], a significant number of patients still suffer from striatal damage despite early diagnosis and treatment, in particular if they are not treated according to recent guideline recommendations [1] [22]. Further, there is strong evidence that extrastriatal changes may increase with age despite early diagnosis and treatment, i.e. in white matter of individuals with a high excretor phenotype [23] [24]. In addition, recent studies report on mass lesions in the white matter reminiscent of tumorigenesis, peripheral polyneuropathy, and the manifestation of chronic renal failure in adulthood [25] [26]. This highlights that chronic toxicity after the vulnerable period of acute and insidious striatal damage is ongoing involving other parts of the brain and other organs. In addition, chronic epigenetic stress induced by enhanced protein glutarylation has been described [27]. All these findings clearly highlight the need for optimization of the current treatment regimen.

2-Aminoadipic and 2-oxoadipic aciduria (OMIM # 204750; Figure 1) is another inborn error of L-lysine degradation. To date, not more than 30 affected individuals have been identified. The spectrum of clinical presentations comprises asymptomatic subjects, mild neurological phenotypes but also severe intellectual disability. Since not all individual with the full biochemical phenotype present with symptoms additional modifiers might be involved. The variable and unspecific presentation could also argue for a sampling bias, since plasma amino acid and urinary organic acid analyses are often performed in patients with neurological abnormalities. However, the causal link between the biochemical and clinical findings is still unclear [28] [29] [30] [31].

We recently elucidated the molecular basis of this disorder using whole exome sequencing [30] and identified pathogenic biallelic mutations in *DHTKD1* (dehydrogenase E1 and transketolase domain containing 1). The genetic association with the biochemical phenotype have been confirmed by [30] and [31]. Moreover, lentiviral overexpression of wildtype *DHTKD1* cDNA in patient fibroblasts rescued the biochemical phenotype confirming that DHTKD1 is indeed involved in the

breakdown of 2-oxoadipate [30]. DHTKD1 is an isoform of 2-oxoglutarate dehydrogenase which in turn is the E1 subunit of 2-oxoglutarate dehydrogenase complex (OGDHc). Our results suggest that DHTKD1 is part of an alternative OGDH-like complex catalyzing the decarboxylation of 2-oxoadipate to glutaryl-CoA [32]. Glutaryl-CoA is substrate of GCDH and precursor of toxic GA and 3-OH-GA. Therefore, we hypothesized that pharmacologic inhibition of DHTKD1 will be a promising novel therapy for GA-I patients. By this strategy, the accumulation of neurotoxic dicarboxylic metabolites of GA-I patients should be reduced or even prevented. A similar approach has been established for tyrosinemia type I caused by inherited deficiency of fumarylacetoacetase and patients presenting with severe hepatorenal symptoms. Today, application of nitisinone, a reversible inhibitor of 4-hydroxyphenylpyruvate dioxygenase [33], blocking an enzyme located two enzymatic steps proximal of fumarylacetoacetase in the tyrosine catabolic pathway, is the pharmacological gold standard treatment for affected patients.

Abbrevations

2-oxoglutarate dehydrogenase complex (OGDHc), 2-oxoglutarate dehydrogenase-like (OGDHL), 3-Hydroxyglutaric acid (3-OHGA), aminoadipate (AA), dehydrogenase E1 and transketolase domain containing 1 (DHTKD1), glutaric acid (GA), glutaric aciduria type I (GA-I), glutarylcarnitine (CD5), oxoadipic acid (OA), glutary-CoA dehydrogenase (GCDH), gas chromatography/mass spectrometry (GC/MS), transcription activator-like effector nucleases (TALEN),

2. Material and methods

2.1 Generation of *Dhtkd1*$^{-/-}$ mice

Dhtkd1$^{-/-}$ mice were generated using the transcription activator-like effector nucleases (TALEN) approach according to established protocols [34] . The system was designed to introduce mutations in Exon 7 of *Dhtkd1*. Females of the inbred strain FVB were used as embryo donors and mated with C57Bl/6N males. Resulting fertilized oozytes were collected and TALENs injected into the larger (male) pronucleus. Injected embryos were reimplanted into pseudopregnant CD-1 foster mothers, giving birth to animals with a FVB and C57Bl/6N mixed background. Sanger sequencing using the following primers identified a 19bp deletion in mutant animals (fw-ATGATAGCCCATGGCAACTG; rev- GTGGAGAGAGGAGGAGGG).

2.2 Clinical characterization of *Dhtkd1*$^{-/-}$ mice

The SHIRPA protocol (SmithKline Beecham, Harwell, Imperial College, Royal London Hospital, phenotype assessment [35]) was performed to monitor neurobehavioral abnormalities. Its modified scope was used, as suggested by Masuya and colleagues [36]. Locomotor activity was measured by counting quadrants within an arena travelled by an animal within 30 seconds. Body position was scored when placing the animals into a viewing jar. Inactive behavior was scored as 0, active behavior as 1 and excessively active behavior as 2. Occurrence of tremor was analysed by observation of forepaws while lifting the mouse by the tail. Transfer arousal was scored after placing the mouse into the middle of an arena. If the animal showed a prolongued freeze of movement during the first 5 seconds, a 0 was scored. For a brief freeze a 1 was scored and for immediate movement the score 2 was assigned. Touch escape was scored while a finger approached the mouse frontally. When no response was shown at all, a 0 was scored, a response to touch scored as 1 and fleeing prior to touch scored with 2. Grip strength was measured using a grip strength meter in triplicate with either forepaws only or all paws holding onto the grid. Inverted grid analysis was performed until a maximum of 30 seconds. Animals were set onto a standard grid and turned upside down. Falling off the grid was assessed for 30 seconds upon turning of the grid. Balance Beam was measured in

triplicate on beams of 60 cm length and differing shapes with beam 1 (round with 22mm) and beam 2 (rectangular with 7mm diameter).

2.3 High-lysine diet

Animals were set on high-lysine diet at the age of 37.7 days (sd ± 5.4, range 28 to 46 days. L-lysine load varied with either chow containing 4.7% lysine (Harlan Laboratories) to 235 mg (chow) or 376 mg (chow + water) daily intake [19]. Treated animals were sacrificed after 40.4 hrs (sd ± 4.9, range 28 to 50 hrs) on diet depending on their clinical appearance. The experiment was finalized if a critical weight loss of more than 15% was achieved.

2.4 Preparation of tissue homogenates

Mice were sacrificed at postnatal day 40 (± 10 days). Tissues (brain, liver) were withdrawn, chilled on liquid nitrogen immediately and stored at -80 °C. Before preparation, tissues were thawed on ice in RC buffer (0.1 mL per 0.1 mg of tissue) containing 250 mmol/L sucrose, 50 mmol/L KCl, 5 mmol/L MgCl2, 20 mmol/ L Tris/HCl (adjusted to pH 7.4) with a Potter Elvehjem system (Fisher Scientific, Schwerte, Germany) using a size that allows the disruption of cell membranes but not organelles, and subcellular fractions were prepared. For preparation of "mitochondria-enriched" fractions, first cell debris and nuclei were removed by centrifuging the homogenates at 600xg, 4°C for 10 min. Next, the 600xg supernatant was centrifuged 10 min, 4°C at 3,500xg and the pellet used as "mitochondria-enriched" fractions [37]. Protein was determined according to [38] with modifications [39] using bovine serum albumin as a standard.

2.5 Quantitative analysis of glutaric, 2-oxoadipic, and 2-aminoadipic acid

GA, 2-OA, and 2-AA were detected in tissue homogenates from mice using quantitative GC/MS with stable-isotope dilution assay as described by Sham [40] with minor modifications. For liquid-liquid extraction 1000 µL of the suspension were used. Briefly, 10 µL each of 1 mmol/L stable isotope-labeled d_4-GA and d_4-nitrophenol (Cambridge Isotope Laboratories, Inc., Andover, MA, USA) were added as internal standards respectively. Samples were acidified with 300 µL of 5M HCl and after

addition of solid sodium chloride extracted twice with 5 mL ethylacetate each time. The combined ethylacetate fractions were dried over sodium sulfate and then dried down at 40 °C under a stream of nitrogen. Samples were then derivatized with N-methyl-N-(trimethylsilyl)heptafluorobutyramide (MSHFBA, Macherey-Nagel, Düren, Germany) for 1 h at 60 °C. For GC/MS analysis, the quadrupole mass spectrometer MSD 5975A (Agilent, Santa Rosa, CA, USA) was run in the selective ion-monitoring mode with electron impact ionization. Gas chromatographic separation was achieved on a capillary column (DB-5MS, 30 m × 0.25 mm; film thickness: 0.25; J&W Scientific, Folsom, CA, USA) using helium as a carrier gas. A volume of 1 µL of the derivatized sample was injected in splitless mode. GC temperature parameters were 80 °C for 2 min, ramp 50 °C/min to 150 °C, ramp 10°C/min to 300 °C, and hold for 2 min at 300 °C. Injector temperature was set to 280 °C and interface temperature to 290 °C.

Fragment ions for quantification were *m/z* 261 (GA), *m/z* 265 (d_4-GA), *m/z* 302 (2-oxoadipic acid). A dwell time of 50 ms was used. Results were normalized to the total protein content

2.6 Quantitative analysis of glutarylcarnitine

C5DC concentrations were measured in tissue homogenates (600×*g* supernatant) by electronspray ionization tandem mass spectrometry according to a method, which was previously described [13]. In brief, 100 µg tissue samples were added into a single well of a 96-well microtiter filter plate to which 100 µL of a methanol stock solution of internal deuterated standards were added. After 20 min, the samples were centrifuged and the eluate was evaporated to dryness, reconstituted in 60 µL of 3 N HCl/butanol, placed in sealed microtiter plates, and incubated at 65 °C for 15 min. The resulting mixtures were dried, and each residue was finally reconstituted in 100 µL solvent of acetonitrile/water/formic acid (50:50:0.025 v/v/v). A PE 200 autosampler transferred 20 µL of each into the collision cell at a solvent flow rate of 40 µL/min using a PE 200 high performance liquid chromatography pump. All acylcarnitines were measured by positive precursor ion scan of m/z 85 (scan range *m/z*: 225–502) and quantified against appropriate deuterated standards with concentrations expressed as µmol/L.

2.7 Western blot analysis

For western blotting "mitochondria-enriched" fractions from livers (see section 2.4) were used and dissolved in RIPA buffer. Proteins were separated by sodium dodecyl sulfate polyacrylamide gel electrophoresis (SDS–PAGE) and transferred to polyvinylidene fluoride membranes by electroblotting. Western blot analysis was performed with a goat polyclonal antibody generated against human DHTKD1 (diluted in 5% milk in TBST; 1:500) and a horseradish peroxidase conjugated secondary antibody (diluted in 5% milk in TBST; 1:2000), visualized by enhanced chemiluminescence.

2.8 Ethics Statement

Mouse experiments and husbandry comply with the EU Directive 2010/63/EU for animal experiments and were carried out with approval of the responsible animal welfare authority, Regierung von Oberbayern, Germany (reference numbers: 55.2-1-54-2532-159-2015 and 55.2-1-54-2532-31-2014).

3. Results

3.1 Generation of a *Dhtkd1*$^{-/-}$ mouse via TALENs

A *Dhtkd1*$^{-/-}$ mouse was generated using the TALEN approach as described by Wefers [32]. Human mutations were identified in exons 1, 7 and 13 of *DHTKD1* (figure 1, [32]). We targeted exon 7 for a deletion, which was predicted to generate a frame shift and lead to a truncated protein lacking the active site. TALEN-injected offspring mice were genotyped via Sanger sequencing of *Dhtkd1* exon 7. A 19bp deletion was identified in a founder mouse. It is predicted to lead to a premature stop codon at amino acid 431. This *Dhtkd1*$^{-/-}$ mouse genetically resembling the patient variant p.Arg410*, was selected for further characterisation. Dhtkd1 immune-decoration experiments using liver tissue detected Dhtkd1 in control mice, but revealed no signal in the *Dhtkd1*$^{-/-}$ mouse model, confirming the loss of function character of the 19bp deletion (Figure 1).

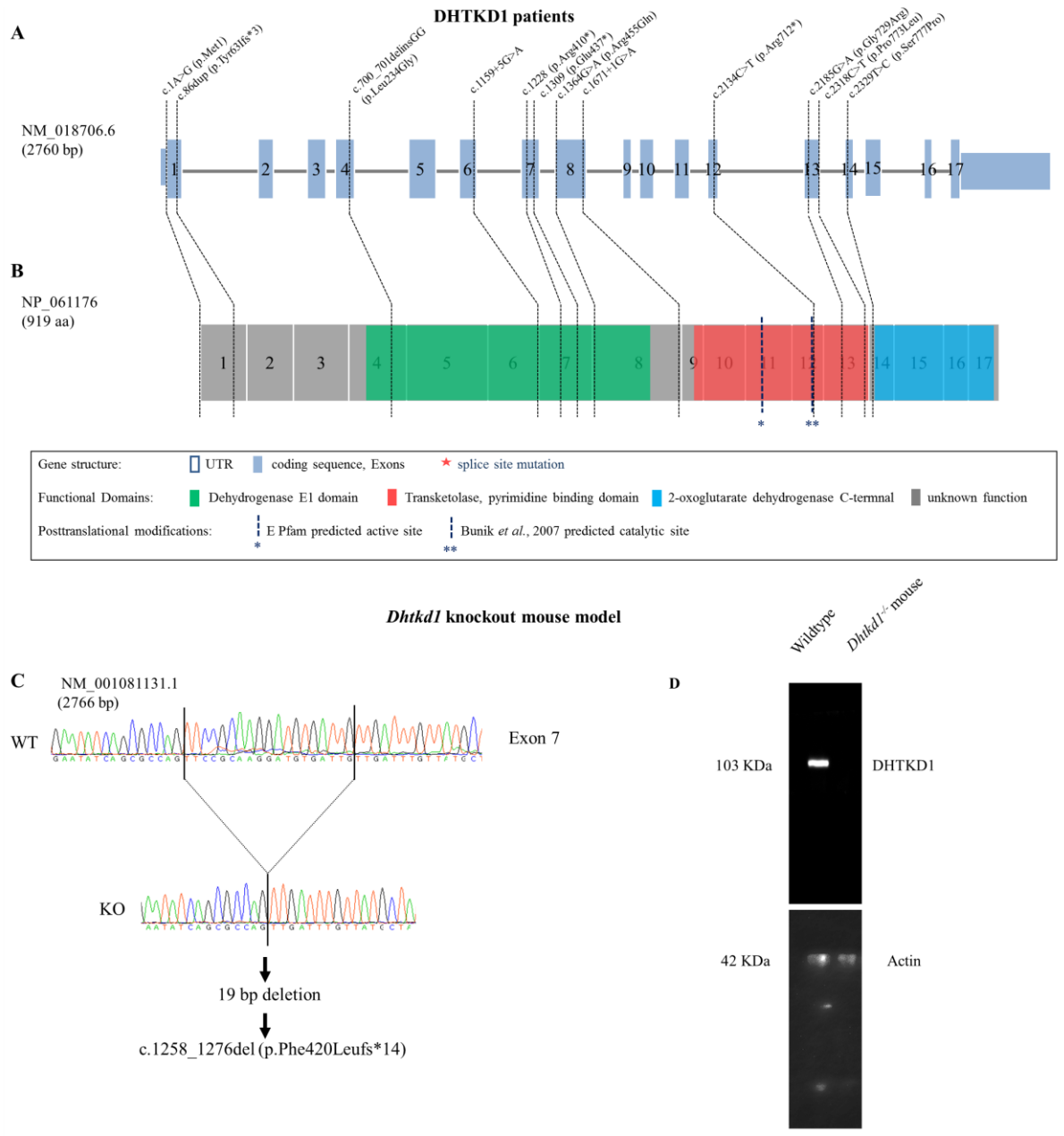

Figure 1: Generation of *Dhtkd1*$^{-/-}$ mice based on human data. A Genomic structure of human *DHTKD1* was taken from the Genome Browser (GRCh38/hg38) with coding exons and UTR's (blue boxes). Known mutations in humans [32] [30] are added at corresponding amino acids. **B** Protein structure of human DHTKD1 with functional domains and posttranslational modifications as predicted by Pfam and Bunik [41]. **C** Sanger sequencing results from a wildtype and a homozygous knockout mouse indicating the 19bp deletion. ExPASy software predicts a premature stop codon at amino acid 431. **D** The blot shows the presence of the Dhtkd1 band in wildtype but not in *Dhtkd1*$^{-/-}$ mouse tissue homogenate. 50 µg of protein was loaded in a 10% gel and β-actin was used as a loading control.

3.2 Characterization of the *Dhtkd1*$^{-/-}$ mouse

To characterize the neuro-behaviour of *Dhtkd1*$^{-/-}$ mice we performed a modified SHIRPA protocol, grip strength analysis, inverted grid and balance beam at the age of 3 months. We did not identify any clinical differences between genotypes (Figure 2). The nominally significant p-value for touch escape is insignificant after correction for multiple testing. Altogether the results are in line with the clinical phenotype of the yet identified DHTKD1 patients and support a mild or asymptomatic presentation. We next asked if the loss of DHTKD1 in mice also leads to the accumulation of 2-OA and 2-AA. Indeed, we found increased 2-OA accumulation in liver of *Dhtkd1* KO, whereas cerebral levels did not differ from control mice (Figure 3). The latter, somewhat unexpected finding is most likely due to the generally very low brain 2-OA levels which are close to the detection limit of our method. In contrast, 2-AA was strongly increased in both tissues (Figure 3C). As expected we could not detect accumulation of GA in liver and brain. In summary, *Dhtkd1*$^{-/-}$ mice reproduce the clinical and biochemical phenotype of affected patients.

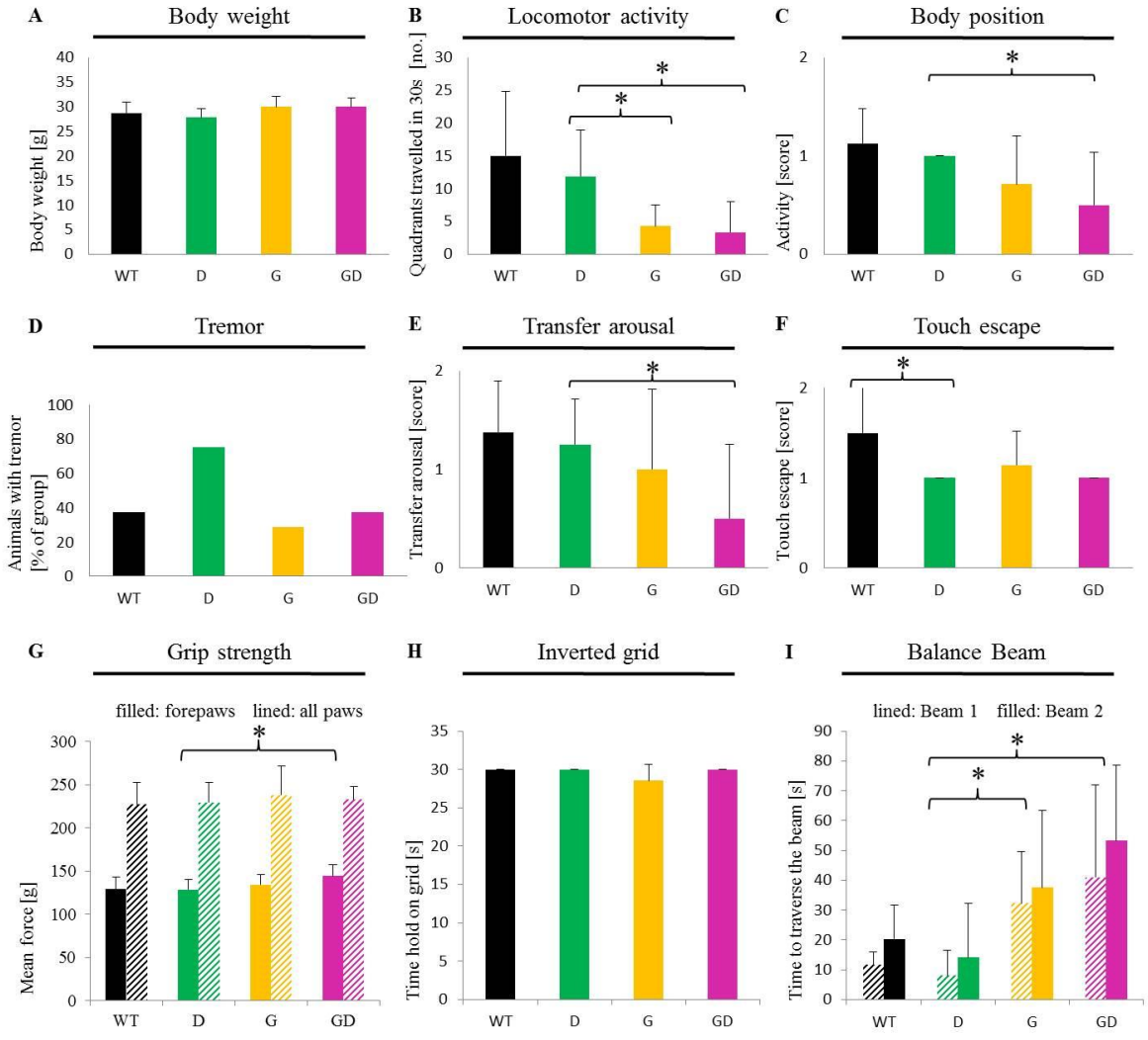

Figure 2: Clinical characterization confirmed non-disease status of *Dhtkd1*$^{-/-}$ in mice. Modified SHIRPA analysis as well as grip strength, inverted grid and balance beam was performed with heterozygous *Dhtkd1*$^{+/-}$ animals as controls (WT=8), homozygous *Dhtkd1*$^{-/-}$ animals (D=8), homozygous *Gcdh*$^{-/-}$ animals (G=7) and double knockout animals (GD=8); n=31 (all male at the age of 3 months). **A)** Body weight, **B)** Locomotor activity, **C)** Body position, **D)** Tremor, **E)** Transfer arousal, **F)** Touch escape, **G)** Grip strength, **H)** Inverted grid **I),** Balance Beam on beam 1 (data 2nd beam not shown but no genotype-specific difference). There were no differences in foot slips, number of falls and stops on neither beam (data not shown). Other observations such as gait, tail elevation, clickbox, trunk curl, limb grasping and urination were without any genotype-specific differences (data not shown). Bars indicate standard deviation; * t-test: $p < 0.05$. Statistically significant differences are indicated between D and all other genotypic groups.

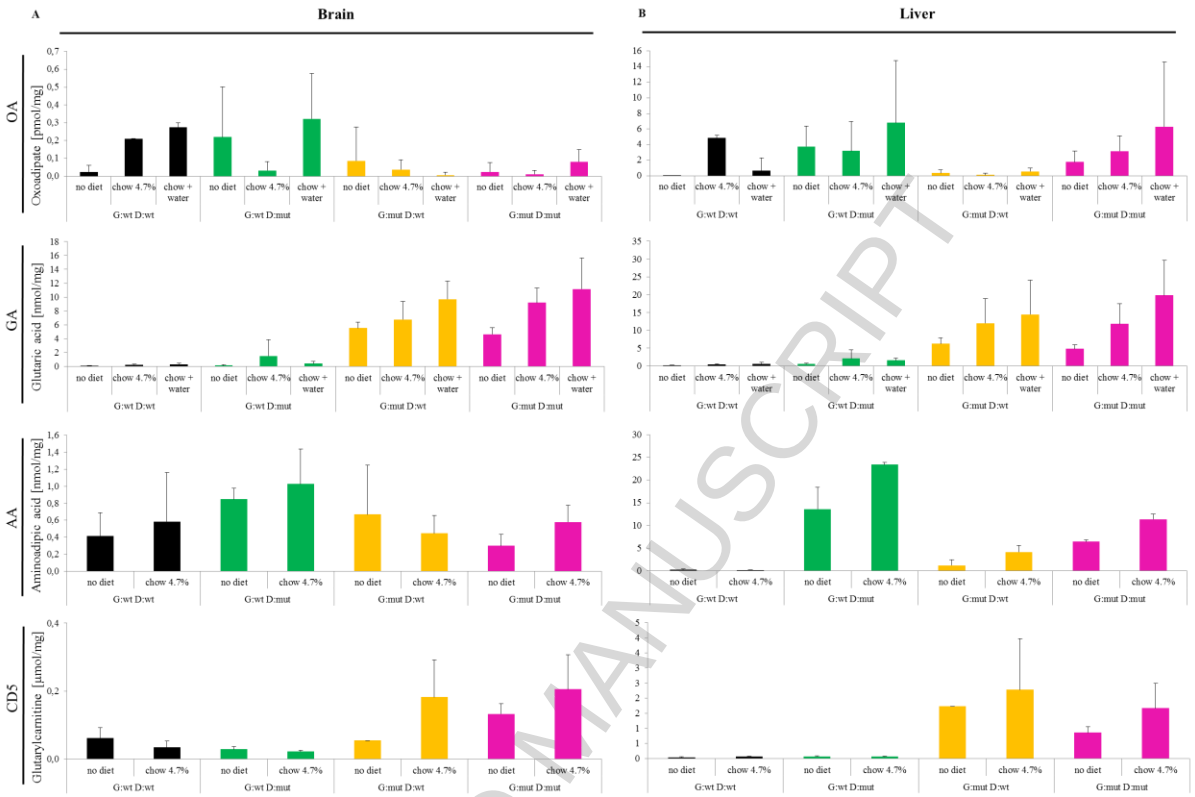

Figure 3: Dhtkd1 knockout results in OA accumulation but does not reduce GA in the *Gcdh*$^{-/-}$ model. Biochemical analyses of *Gcdh*$^{-/-}$/*Dhtkd1*$^{-/-}$ mouse line on normal or high-lysine diet compared to wildtype and single knock-out lines**.** Oxoadipate (OA), glutaric acid (GA), aminoadipic acid (AA) and glutarylcarnitine (CD5) levels are described in A) brain tissue and B) liver tissue. No diet = normal diet (age of 39.2 days (sd ± 7.7)); chow 4.7% = high lysine in chow (age of 39.7 days (sd ± 3.5)); chow+water = high lysine in chow and water (age of 36.2 days (sd ± 4.8)); G= Gcdh, D= Dhtkd1, n≥5 for GA and OA; n=3-4 for AA and CD5; bars indicate standard deviation.

3.3 Generation and characterization of *Dhtkd1*$^{-/-}$/*Gcdh*$^{-/-}$ mice

In order to test whether inhibition of Dhtkd1 can attenuate the Gcdh knockout phenotype, the well characterised Gcdh deficient mouse line [16] was crossed with the newly generated *Dhtkd1*$^{-/-}$ line. After several generations of inbreeding, we obtained double knockout animals homozygous for both *Dhtkd1* and *Gcdh*. The resulting mice harboured a mixed genetic background based on C57Bl/6 (37.5%), FVB (12.5%) and Sv129 (50%). We next generated age-matched animals of four different genotypes, i.e. *Dhtkd1*$^{+/+}$/*Gcdh*$^{+/+}$, *Dhtkd1*$^{-/-}$/*Gcdh*$^{+/+}$, *Dhtkd1*$^{+/+}$/*Gcdh*$^{-/-}$, and *Dhtkd1*$^{-/-}$/*Gcdh*$^{-/-}$. Under standard conditions we observed a clinical phenotype in *Dhtkd1*$^{+/+}$/*Gcdh*$^{-/-}$ and *Dhtkd1*$^{-/-}$/*Gcdh*$^{-/-}$ mice at 3 months of age (figure 2). After correction for multiple testing, only *Gcdh*$^{-/-}$ animals are

significantly slower than *Dhtkd1*$^{-/-}$ and WT at traversing a beam. When following the mouse lines (n=375 animals of different genotypes) until the age of 180 days, we did not detect any signs of illness in the cohort. After a mean age of 250 days, only one (*Dhtkd1*$^{-/-}$/*Gcdh*$^{-/+}$) died at 214 days (data not shown).

3.4 Dhtkd1 knockout is not able to rescue the clinical phenotype of Gcdh deficient mice

In *Gcdh*$^{-/-}$ mice, a clinical and more pronounced biochemical phenotype can be induced by increased lysine diet [19] [18]. To test our hypothesis that Dhtkd1 knockout rescues the clinical and biochemical phenotype of Gcdh deficiency, we followed three treatment regimens; normal diet, diet with 4.7% lysine in chow, and diet with 4.7% lysine in both water and chow according to a previous study [19]. Weight change upon diet was defined as primary and behavioral abnormality as secondary clinical outcome measure. 24 hours after the start of diet none of the wildtype, one of seven *Dhtkd1*$^{-/-}$ mice, but four of five *Gcdh*$^{-/-}$ mice displayed the critical weight loss of more than 15% [19]. Unexpectedly, all double knockout mice (7/7) showed critical weight loss within 24 hrs resembling *Gcdh*$^{-/-}$ mice. Behavioral abnormality presented as extreme passivity. As depicted in figure 4B, almost all *Gcdh*$^{-/-}$ (4/5) and *Dhtkd1*$^{-/-}$/*Gcdh*$^{-/-}$ (5/6) showed lethargic behavior after 24 hrs on high-lysine diet, whereas only one wildtype (1/7) and two Dhtkd1 knockout animals (2/7) displayed behavioral abnormalities. In summary, double knockout mice showed the same vulnerability for increased dietary lysine supply as *Gcdh*$^{-/-}$ mice being in strong contrast to our initial hypothesis.

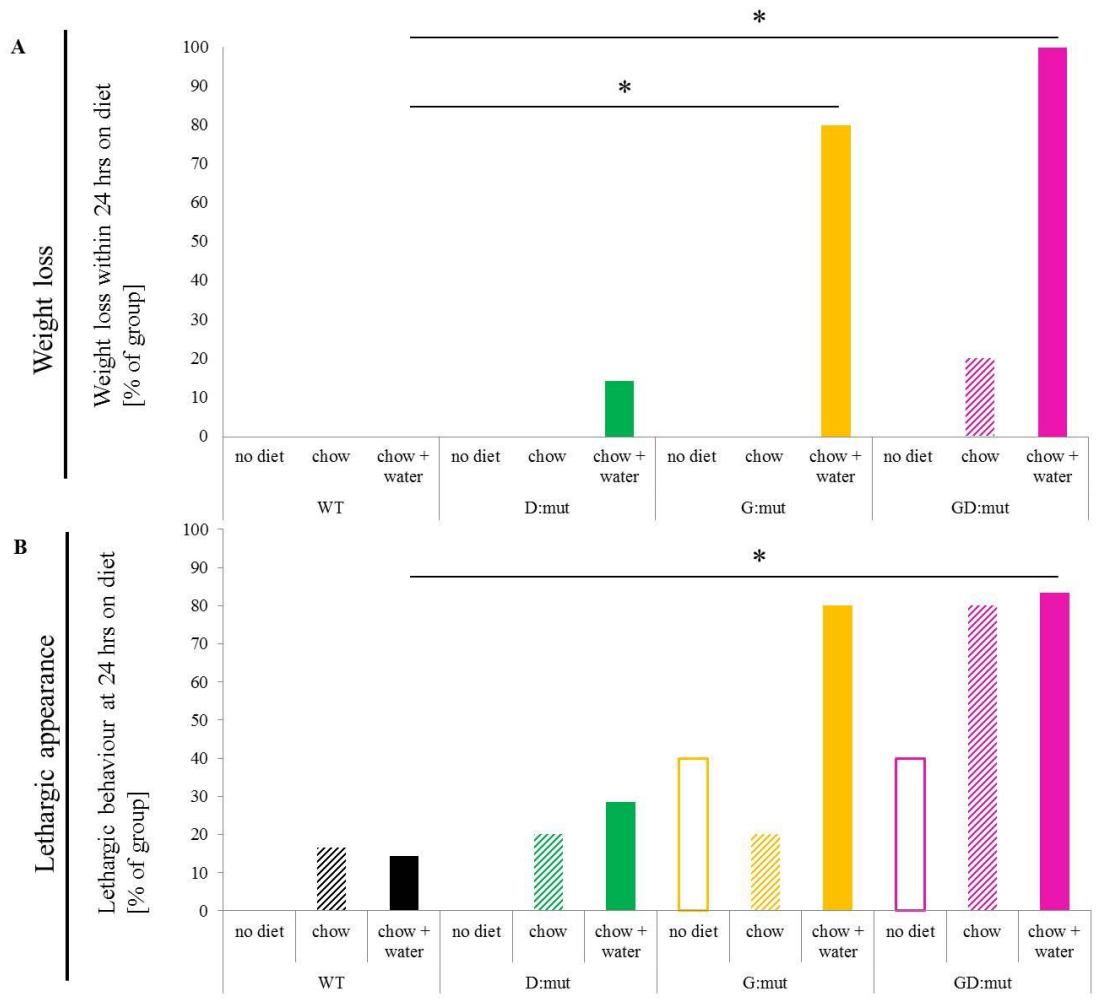

Figure 4: Clinical analysis of *Dhtkd1*$^{-/-}$/*Gcdh*$^{-/-}$ mice on low versus high-lysine diet. Clinical analysis at 24 hrs after start of diet with high-lysine in chow or in chow and water from four different genotypes; A) Critical weight loss within 24 hrs was achieved at >15 % loss as compared to diet start. B) Lethargic behaviour was assigned when animals, put into an arena moved less than 2 quadrants within 30 s. (no diet/ high-lysine in chow/ high-lysine in chow and water). WT = *Gcdh*$^{+/+}$/*Dhtkd1*$^{+/+}$ (n = 8/6/7); D:mut = *Gcdh*$^{+/+}$/*Dhtkd1*$^{-/-}$ (n = 5/5/7); G:mut = *Gcdh*$^{-/-}$/*Dhtkd1*$^{+/+}$ (n = 5/5/5); GD:mut = *Gcdh*$^{-/-}$/*Dhtkd1*$^{-/-}$ (n = 5/5/6). *Fisher's Exact test: $p < 0.05$.

3.5 Dhtkd1 knockout does not prevent GA accumulation due to Gcdh deficiency

We next asked if the undistinguishable clinical presentation of both *Gcdh*$^{-/-}$ and *Gcdh*$^{-/-}$/*Dhtkd1*$^{-/-}$ mice was also reflected on the metabolic level or might be due to an unexpected interaction of the two loss of function mutations. To this end we prepared tissue homogenates (liver and brain) of mice (genotypes, *Dhtkd1*$^{+/+}$/*Gcdh*$^{+/+}$, *Dhtkd1*$^{-/-}$/*Gcdh*$^{+/+}$, *Dhtkd1*$^{+/+}$/*Gcdh*$^{-/-}$, and *Dhtkd1*$^{-/-}$/*Gcdh*$^{-/-}$) under standard and high lysine diets and determined GA, 2-OA, and 2-AA levels. 2-OA was increased in *Dhtkd1*$^{-/-}$ and *Gcdh*$^{-/-}$/*Dhtkd1*$^{-/-}$ mice. 2-AA was accumulating in *Dhtkd1*$^{-/-}$ and *Gcdh*$^{-/-}$/*Dhtkd1*$^{-/-}$ mice

on a standard diet and increasing with dietary lysine supply (Figure 3C). As described before [19] [18], we confirm that increased dietary lysine supply results in a further rise of GA levels in *Gcdh*$^{-/-}$ mice (Figure 3). This effect was not found in wildtype or Dhtkd1 deficient mice. In line with the same clinical phenotype of *Dhtkd1*$^{-/-}$*/Gcdh*$^{-/-}$ and *Gcdh*$^{-/-}$ *mice* on high lysine diet, both animal models displayed increased and comparable GA levels in liver and, more importantly, brain. Moreover, we even found similar GA levels in *Dhtkd1*$^{-/-}$*/Gcdh*$^{-/-}$ and *Gcdh*$^{-/-}$ *mice* on a standard diet. CD5 is used in newborn screening as metabolic marker for GA-I and initiates the physiological detoxification route of accumulating glutaryl-CoA. Indeed, also CD5 was increased in *Dhtkd1*$^{-/-}$*/Gcdh*$^{-/}$ mice under high lysine (Figure 3). This observation further underlines that loss of Dhtkd1 activity does not rescue Gcdh deficiency, neither on biochemical nor clinical level.

4. Discussion

GA-I is an inborn defect of lysine, hydroxylysine and tryptophan metabolism resulting in the accumulation of neurotoxic GA and 3-OH-GA as well as glutaryl-CoA. Lysine is the quantitatively most relevant precursor of these metabolites [17] [18]. The current treatment regimen for GA-I aims to reduce the accumulation of toxic metabolites by low lysine diet, carnitine supplementation and, on demand, emergency treatment [1] [20]. Safety and efficacy of this metabolic treatment has been shown in patients and *Gcdh*$^{-/-}$ mice [21] [1]. However, some early diagnosed and treated patients still suffer from striatal damage, and extrastriatal changes poorly respond to the current treatment [23] [24]. Subependymal mass lesions reminiscent of tumorigenesis, peripheral polyneuropathy, and the manifestation of chronic renal failure [25] [26] [42] indicate that the disease course does not halt in adults but involves other parts of the brain and additional organs. In total, there is a clear need for optimization of the current treatment regimen which we aimed to address in our study.

We have recently identified mutations of the *DHTKD1* gene in patients with 2-aminoadipic and 2-oxoadipic aciduria, a defect in lysine metabolism upstream of GA-I, which can be tolerated in a number of individuals without a severe clinical impairment [30] [31] [32]. Inspired by the treatment of tyrosinaemia type 1, which blocks toxic metabolite production by pharmacological inhibition of an upstream enzyme (4-hydroxyphenylpyruvate dioxygenase by nitisinone), we postulated that inhibition of DHTKD1 will prevent toxic metabolite production in GA-I. To test this hypothesis we generated *Dhtkd1*$^{-/-}$*/Gcdh*$^{+/+}$ and *Dhtkd1*$^{-/-}$*/Gcdh*$^{-/-}$ mice using the TALEN technology and compared their biochemical and clinical phenotype with *Dhtkd1*$^{+/+}$*/Gcdh*$^{-/-}$ and *Dhtkd1*$^{+/+}$*/Gcdh*$^{+/+}$ mice. The phenotype of *Dhtkd1*$^{-/-}$*/Gcdh*$^{+/+}$ mice was similar to the one of patients with 2-aminoadipic and 2-oxoadipic aciduria showing increased 2-OA and 2-AA accumulation without a clear clinical phenotype [28] [29] [32]. *Gcdh*$^{-/-}$ mice do not develop spontaneous neurological disease but stimulation of toxic metabolite production by high lysine diet induces brain damage similar to affected patients ultimately leading to death [19] [18]. Symptomatic mice typically show lethargy and dramatic weight loss within 48 h of treatment start. We therefore defined these two parameters as clinical and GA accumulation as biochemical endpoints in our study. Unexpectedly, increased dietary

lysine supply induced lethargy and weight loss to the same extent in *Dhtkd1*$^{+/+}$*/Gcdh*$^{-/-}$ and *Dhtkd1*$^{-/-}$*/Gcdh*$^{-/-}$ mice. In line with the toxic metabolite hypothesis, both mouse models were characterized by elevated GA levels on a standard diet which were strongly boosted by the high lysine diet. Carnitine conjugation is an endogenous route to detoxify accumulating CoA-esters. Similar glutarylcarnitine levels in *Dhtkd1*$^{-/-}$*/Gcdh*$^{-/-}$ and *Dhtkd1*$^{+/+}$*/Gcdh*$^{-/-}$ mice indicate that in both models glutaryl-CoA is formed and is a precursor of GA. In summary our data suggests that loss of function mutations in *Dhtkd1* do not rescue the clinical and biochemical phenotype of Gcdh deficiency. Furthermore, this also challenges our current understanding of lysine metabolism.

Our data suggests at least a second way to form glutaryl-CoA from L-Lysine. L-Lysine oxidation (Figure 5) is a complex and yet not completely unravelled metabolic pathway. In mammals, the first steps of mitochondrial L-lysine oxidation are catalysed by the bifunctional enzyme 2-aminoadipate semialdehyde synthase (AASS) being localized in the mitochondrial matrix [43]. An alternative route via the pipecolate pathway has been postulated to initiate lysine oxidation in brain [17] [44] [45] [46] [47]. Both pathways are suggested to converge in 2-aminoadipate semialdehyde, which is further metabolized by 2-aminoadipate semialdehyde dehydrogenase (AASDH) and 2-aminoadipate aminotransferase in 2-oxoadipate (AADAT; [48]). However, two recent publications challenge this concept. The mitochondrial pathway is initiated by ε-deamination of lysine, whereas the peroxisomal route requires removal of the ammonia group in α-position. Two recent studies accordingly showed that in mice injection of L-[α-^{15}N]lysine leads to enrichment of L-[α-^{15}N]aminoadipate and of L-[ε-^{15}N]lysine to enrichment of L-[ε-^{15}N]pipecolate - in liver and brain [49] [50]. However, both studies failed to detect L-[ε-^{15}N]aminoadipate which would be produced if mitochondrial and peroxisomal lysine degradation indeed converged in 2-aminoadipate semialdehyde suggesting that L-pipecolate is further metabolized by a yet unknown pathway [49] [50] – which could ultimately result in GA formation. Finally, conversion of 2-oxoadipate to glutaryl-CoA is thought to be catalysed by an alternative 2-oxoglutarate dehydrogenase complex containing DHTKD1 (OGDHc-like; [32]). OGDHc has also been shown to catalyze this reaction, though its affinity to 2-oxoadipate is three times lower compared to 2-oxoglutarate [17] [51] [52]. Moreover, there is a third

paralog of the E1 subunit, OGDHL [41]. Little is known about this protein; it is highly expressed in brain and has similar substrate specificity as OGDH.

Based on the aforementioned lysine metabolism pathway, GA in *Dhtkd1*$^{-/-}$/*Gcdh*$^{-/-}$ mice may derive from the pipecolate pathway or, alternately, OGDHc or OGDHL may substitute for the loss of DHTKD1 activity. The pipecolate pathway is at least in liver of minor importance and no up-regulation has been found in *Gcdh*$^{-/-}$ mice [49], which could explain the unchanged GA levels in *Dhtkd1*$^{-/-}$/*Gcdh*$^{-/-}$ mice. Moreover, we did not observe an increase of hepatic L-pipecolate levels in *Dhtkd1*$^{-/-}$/*Gcdh*$^{-/-}$ mice (0.2 ± 0.05 nmol/mg protein) in comparison to *Dhtkd*$^{-/-}$/*Gcdh*$^{+/+}$ or *Dhtkd1*$^{+/+}$/*Gcdh*$^{+/+}$ mice (0.11 ± 0.07 and 0.20 ± 0.06 nmol/mg protein respectively) if fed a high lysine diet. This finding speaks against the pipecolate pathway proving precursors for GA synthesis.

Glutaric aciduria type 3 is a nondisease also characterized by GA accumulation due to pathogenic mutations of succinyl-CoA:glutarate-CoA transferase [53]. In contrast to GA-I, patients do not display elevated glutarylcarnitine levels indicating that GA is directly produced in a yet unknown metabolic pathway omitting the step of CoA-conjugation or may derive from gut bacteria. This finding led to the conclusion that the pathomechanism in GA-I is indeed linked to increased glutaryl-CoA generation. Accumulation of glutarylcarnitine in combination with the severe clinical phenotype of *Dhtkd1*$^{-/-}$/*Gcdh*$^{-/-}$ mice on a high lysine diet therefore speak in favour of OGDHc or OGDHc containing OGDHL, at least partially replacing the loss of function of DHTKD1. The accumulation of 2-AA and 2-OA in *Dhtkd1*$^{-/-}$ mice is mild compared to GA levels in *Gcdh*$^{-/-}$ mice, suggesting that there is indeed an alternative route partly bypassing the defect Dhtkd1 complex. Our results suggest, that as a therapeutic approach, pharmacologic inhibition of Dhtkd1 is not sufficient in GA-I patients to prevent the manifestation of brain damage. Instead, a more complex approach is required.

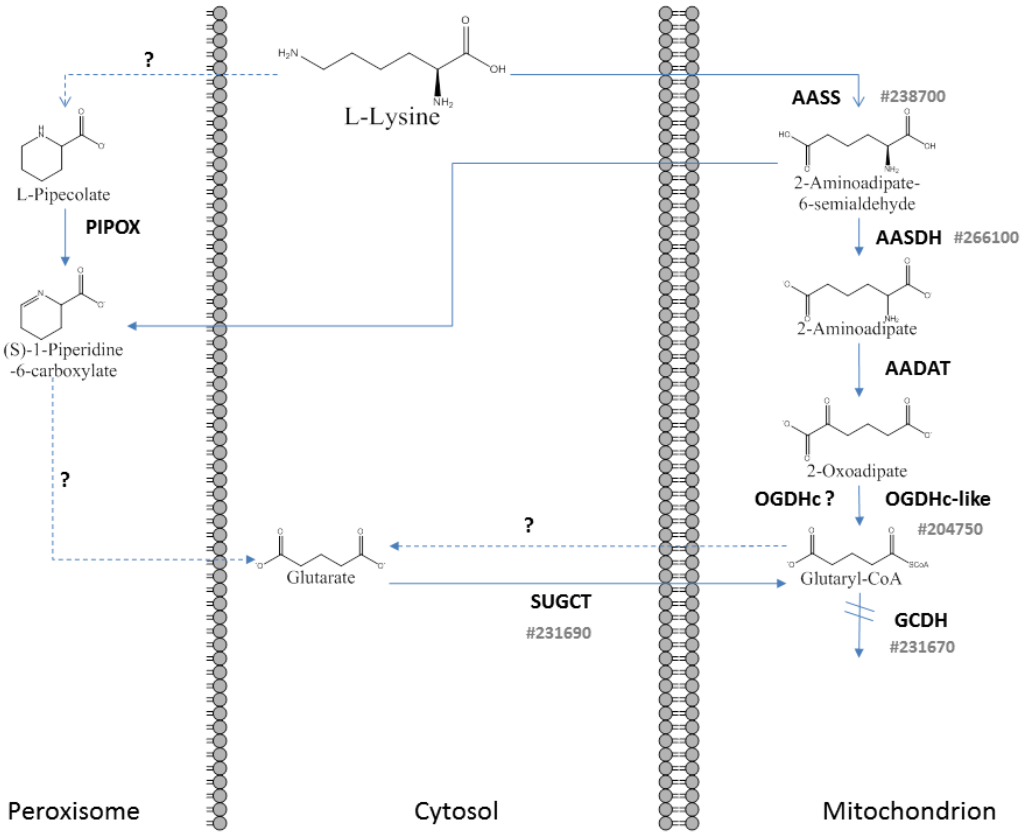

Figure 5 Synopsis of L-lysine metabolism. Mammalian L-lysine oxidation can start with the mitochondrial bifunctional enzyme 2-aminoadipate semialdehyde synthase (AASS) [43] or happen in the peroxisomal pipecolate pathway [17] [44] [45] [46]. Both pathways are thought to converge in 2-aminoadipate semialdehyde, which is further metabolized by 2-aminoadipate semialdehyde dehydrogenase (AASDH) and 2-aminoadipate aminotransferase in 2-oxoadipate (AADAT). Two recent studies challenge this notion [49] [50] and suggest that L-pipecolate is further metabolized by a yet unknown pathway which may lead to GA production. 2-Oxoadipate can be converted to glutaryl-CoA by a) 2-oxoglutarate dehydrogenase complex containing DHTKD1 (OGDHc-like; [32]), b) by OGDHc though with a three times lower substrate affinity compared to 2-oxoglutarate [17], or c) OGDHL [41] a yet poorly studied paralogue of OGDH. GA itself can be converted to glutaryl-CoA by succinyl-CoA:glutarate-CoA transferase (SUGCT). If applicable, OMIM numbers are depicted next to the respective enzyme; OMIM #238700 – hyperlysinemia type I, #266100 – pyridoxine dependent epilepsy, #204750 – 2-aminoadipic 2-oxoadipic aciduria, #231670 – glutaric aciduria I; #231690 – glutaric aciduria III.

Funding

This work was supported by the Deutsche Forschungsgemeinschaft [grant number SA 1970/4-1, KO 2010/8-1, and PR 668/2-1)

5. References

[1] J. Heringer, S. Boy, R. Ensenauer, B. Assmann, J. Zschocke, I. Harting, T. Lücke, E.M. Maier, C. Mühlhausen, G. Haege, Use of guidelines improves the neurological outcome in glutaric aciduria type I, Ann. Neurol., 68 (2010) 743-752.

[2] A.A. Basinger, J.K. Booker, D.M. Frazier, D.D. Koeberl, J.A. Sullivan, J. Muenzer, Glutaric acidemia type 1 in patients of Lumbee heritage from North Carolina, Mol. Genet. Metab., 88 (2006) 90-92.

[3] C. Greenberg, A. Prasad, L. Dilling, J. Thompson, J. Haworth, B. Martin, P. Wood-Steiman, L. Seargeant, B. Seifert, F. Booth, Outcome of the first 3-years of a DNA-based neonatal screening program for glutaric acidemia type 1 in Manitoba and northwestern Ontario, Canada, Mol. Genet. Metab., 75 (2002) 70-78.

[4] E. Naughten, P. Mayne, A. Monavari, S. Goodman, G. Sulaiman, D. Croke, Glutaric aciduria type I: outcome in the Republic of Ireland, J. Inherit. Metab. Dis., 27 (2004) 917-920.

[5] K.A. Strauss, E.G. Puffenberger, D.L. Robinson, D.H. Morton, Type I glutaric aciduria, part 1: natural history of 77 patients, Am. J. Med. Genet. C Semin. Med. Genet., 121C (2003) 38-52.

[6] G. van der Watt, E.P. Owen, P. Berman, S. Meldau, N. Watermeyer, S.E. Olpin, N.J. Manning, I. Baumgarten, F. Leisegang, H. Henderson, Glutaric aciduria type 1 in South Africa-high incidence of glutaryl-CoA dehydrogenase deficiency in black South Africans, Mol. Genet. Metab., 101 (2010) 178-182.

[7] S. Kölker, S.F. Garbade, C.R. Greenberg, J.V. Leonard, J.M. Saudubray, A. Ribes, H.S. Kalkanoglu, A.M. Lund, B. Merinero, M. Wajner, M. Troncoso, M. Williams, J.H. Walter, J. Campistol, M. Marti-Herrero, M. Caswill, A.B. Burlina, F. Lagler, E.M. Maier, B. Schwahn, A. Tokatli, A. Dursun, T. Coskun, R.A. Chalmers, D.M. Koeller, J. Zschocke, E. Christensen, P. Burgard, G.F. Hoffmann, Natural history, outcome, and treatment efficacy in children and adults with glutaryl-CoA dehydrogenase deficiency, Pediatr. Res., 59 (2006) 840-847.

[8] S. Kölker, G. Köhr, B. Ahlemeyer, J.G. Okun, V. Pawlak, F. Hörster, E. Mayatepek, J. Krieglstein, G.F. Hoffmann, Ca2+ and Na+ Dependence of 3-Hydroxyglutarate-Induced Excitotoxicity in Primary Neuronal Cultures from Chick Embryo Telencephalons, Pediatr. Res., 52 (2002) 199-206.

[9] S. Kölker, D.M. Koeller, J.G. Okun, G.F. Hoffmann, Pathomechanisms of neurodegeneration in glutaryl-CoA dehydrogenase deficiency, Ann. Neurol., 55 (2004) 7-12.

[10] S.W. Sauer, J.G. Okun, M.A. Schwab, L.R. Crnic, G.F. Hoffmann, S.I. Goodman, D.M. Koeller, S. Kölker, Bioenergetics in Glutaryl-Coenzyme A Dehydrogenase Deficiency A ROLE FOR GLUTARYL-COENZYME A, J. Biol. Chem., 280 (2005) 21830-21836.

[11] J. Lamp, B. Keyser, D.M. Koeller, K. Ullrich, T. Braulke, C. Muhlhausen, Glutaric aciduria type 1 metabolites impair the succinate transport from astrocytic to neuronal cells, J. Biol. Chem., 286 (2011) 17777-17784.

[12] K.A. Strauss, P. Donnelly, M. Wintermark, Cerebral haemodynamics in patients with glutaryl-coenzyme A dehydrogenase deficiency, Brain, 133 (2010) 76-92.

[13] S.W. Sauer, J.G. Okun, G. Fricker, A. Mahringer, I. Müller, L.R. Crnic, C. Mühlhausen, G.F. Hoffmann, F. Hörster, S.I. Goodman, Intracerebral accumulation of glutaric and 3-hydroxyglutaric acids secondary to limited flux across the blood–brain barrier constitute a biochemical risk factor for neurodegeneration in glutaryl-CoA dehydrogenase deficiency, J. Neurochem., 97 (2006) 899-910.

[14] S.W. Sauer, S. Opp, A. Mahringer, M.M. Kaminski, C. Thiel, J.G. Okun, G. Fricker, M.A. Morath, S. Kölker, Glutaric aciduria type I and methylmalonic aciduria: simulation of cerebral import and export of accumulating neurotoxic dicarboxylic acids in in vitro models of the blood-brain barrier and the choroid plexus, Biochim. Biophys. Acta, 1802 (2010) 552-560.

[15] S. Kölker, S. Sauer, R. Surtees, J. Leonard, The aetiology of neurological complications of organic acidaemias—a role for the blood–brain barrier, J. Inherit. Metab. Dis., 29 (2006) 701-704.

[16] D.M. Koeller, M. Woontner, L.S. Crnic, B. Kleinschmidt-DeMasters, J. Stephens, E.L. Hunt, S.I. Goodman, Biochemical, pathologic and behavioral analysis of a mouse model of glutaric acidemia type I, Hum. Mol. Genet., 11 (2002) 347-357.

[17] S.W. Sauer, S. Opp, G.F. Hoffmann, D.M. Koeller, J.G. Okun, S. Kölker, Therapeutic modulation of cerebral L-lysine metabolism in a mouse model for glutaric aciduria type I, Brain, 134 (2011) 157-170.

[18] W.J. Zinnanti, J. Lazovic, C. Housman, K. LaNoue, J.P. O'Callaghan, I. Simpson, M. Woontner, S.I. Goodman, J.R. Connor, R.E. Jacobs, Mechanism of age-dependent susceptibility and novel treatment strategy in glutaric acidemia type I, The Journal of clinical investigation, 117 (2007) 3258-3270.

[19] S.W. Sauer, S. Opp, S. Komatsuzaki, A.-E. Blank, M. Mittelbronn, P. Burgard, D. Koeller, J.G. Okun, S. Kölker, Multifactorial modulation of susceptibility to l-lysine in an animal model of glutaric aciduria type I, Biochimica et Biophysica Acta (BBA)-Molecular Basis of Disease, 1852 (2015) 768-777.

[20] S. Kölker, S.F. Garbade, N. Boy, E.M. Maier, T. Meissner, C. Mühlhausen, J.B. Hennermann, T. Lücke, J. Häberle, J. Baumkötter, Decline of acute encephalopathic crises in children with glutaryl-CoA dehydrogenase deficiency identified by newborn screening in Germany, Pediatr. Res., 62 (2007) 357-363.

[21] N. Boy, G. Haege, J. Heringer, B. Assmann, C. Mühlhausen, R. Ensenauer, E.M. Maier, T. Lücke, G.F. Hoffmann, E. Müller, Low lysine diet in glutaric aciduria type I–effect on anthropometric and biochemical follow-up parameters, J. Inherit. Metab. Dis., 36 (2013) 525-533.

[22] S. Kölker, E. Christensen, J.V. Leonard, C.R. Greenberg, A. Boneh, A.B. Burlina, A.P. Burlina, M. Dixon, M. Duran, A.G. Cazorla, Diagnosis and management of glutaric aciduria type I–revised recommendations, J. Inherit. Metab. Dis., 34 (2011) 677-694.

[23] I. Harting, E. Neumaier-Probst, A. Seitz, E.M. Maier, B. Assmann, I. Baric, M. Troncoso, C. Mühlhausen, J. Zschocke, N.P. Boy, Dynamic changes of striatal and extrastriatal abnormalities in glutaric aciduria type I, Brain, 132 (2009) 1764-1782.

[24] I. Harting, N. Boy, J. Heringer, A. Seitz, M. Bendszus, P.J. Pouwels, S. Kölker, 1H-MRS in glutaric aciduria type 1: impact of biochemical phenotype and age on the cerebral accumulation of neurotoxic metabolites, J. Inherit. Metab. Dis., 38 (2015) 829-838.

[25] M. Herskovitz, D. Goldsher, B.-A. Sela, H. Mandel, Subependymal mass lesions and peripheral polyneuropathy in adult-onset glutaric aciduria type I, Neurology, 81 (2013) 849-850.

[26] S. Kölker, V. Valayannopoulos, A.B. Burlina, J. Sykut-Cegielska, F.A. Wijburg, E.L. Teles, J. Zeman, C. Dionisi-Vici, I. Barić, D. Karall, The phenotypic spectrum of organic acidurias and urea cycle disorders. Part 2: the evolving clinical phenotype, J. Inherit. Metab. Dis., 38 (2015) 1059-1074.

[27] M. Tan, C. Peng, K.A. Anderson, P. Chhoy, Z. Xie, L. Dai, J. Park, Y. Chen, H. Huang, Y. Zhang, Lysine glutarylation is a protein posttranslational modification regulated by SIRT5, Cell Metab., 19 (2014) 605-617.

[28] H. Przyrembel, D. Bachmann, I. Lombeck, K. Becker, U. Wendel, S. Wadman, H. Bremer, Alpha-ketoadipic aciduria, a new inborn error of lysine metabolism; biochemical studies, Clin. Chim. Acta, 58 (1975) 257-269.

[29] M. Duran, F. Beemer, S. Wadman, U. Wendel, B. Janssen, A patient with α-ketoadipic and α-aminoadipic aciduria, J. Inherit. Metab. Dis., 7 (1984) 61-61.

[30] J. Hagen, H. te Brinke, R.J. Wanders, A.C. Knegt, E. Oussoren, A.J.M. Hoogeboom, G.J. Ruijter, D. Becker, K.O. Schwab, I. Franke, Genetic basis of alpha-aminoadipic and alpha-ketoadipic aciduria, J. Inherit. Metab. Dis., 38 (2015) 873-879.

[31] A.R. Stiles, L. Venturoni, G. Mucci, N. Elbalalesy, M. Woontner, S. Goodman, J.E. Abdenur, New Cases of DHTKD1 Mutations in Patients with 2-Ketoadipic Aciduria, JIMD Reports, Volume 25, Springer, Place Published, 2015, pp. 15-19.

[32] K. Danhauser, S.W. Sauer, T.B. Haack, T. Wieland, C. Staufner, E. Graf, J. Zschocke, T.M. Strom, T. Traub, J.G. Okun, DHTKD1 mutations cause 2-aminoadipic and 2-oxoadipic aciduria, The American Journal of Human Genetics, 91 (2012) 1082-1087.

[33] S. Lindstedt, E. Holme, E. Lock, O. Hjalmarson, B. Strandvik, Treatment of hereditary tyrosinaemia type I by inhibition of 4-hydroxyphenylpyruvate dioxygenase, The Lancet, 340 (1992) 813-817.

[34] B. Wefers, M. Meyer, O. Ortiz, M.H. de Angelis, J. Hansen, W. Wurst, R. Kühn, Direct production of mouse disease models by embryo microinjection of TALENs and oligodeoxynucleotides, Proceedings of the National Academy of Sciences, 110 (2013) 3782-3787.

[35] D.C. Rogers, E. Fisher, S. Brown, J. Peters, A. Hunter, J. Martin, Behavioral and functional analysis of mouse phenotype: SHIRPA, a proposed protocol for comprehensive phenotype assessment, Mamm. Genome, 8 (1997) 711-713.

[36] H. Masuya, M. Inoue, Y. Wada, A. Shimizu, J. Nagano, A. Kawai, A. Inoue, T. Kagami, T. Hirayama, A. Yamaga, Implementation of the modified-SHIRPA protocol for screening of dominant phenotypes in a large-scale ENU mutagenesis program, Mamm. Genome, 16 (2005) 829-837.

[37] M.M. Kaminski, S.W. Sauer, M. Kaminski, S. Opp, T. Ruppert, P. Grigaravicius, P. Grudnik, H.J. Grone, P.H. Krammer, K. Gulow, T cell activation is driven by an ADP-dependent glucokinase linking enhanced glycolysis with mitochondrial reactive oxygen species generation, Cell Rep, 2 (2012) 1300-1315.

[38] O.H. Lowry, N.J. Rosebrough, A.L. Farr, R.J. Randall, Protein measurement with the Folin phenol reagent, J. Biol. Chem., 193 (1951) 265-275.

[39] A. Helenius, K. Simons, The binding of detergents to lipophilic and hydrophilic proteins, J. Biol. Chem., 247 (1972) 3656-3661.

[40] F. Sahm, D. Capper, S. Pusch, J. Balss, A. Koch, C.D. Langhans, J.G. Okun, A. von Deimling, Detection of 2-Hydroxyglutarate in Formalin-Fixed Paraffin-Embedded Glioma Specimens by Gas Chromatography/Mass Spectrometry, Brain Pathol., 22 (2012) 26-31.

[41] V. Bunik, T. Kaehne, D. Degtyarev, T. Shcherbakova, G. Reiser, Novel isoenzyme of 2-oxoglutarate dehydrogenase is identified in brain, but not in heart, FEBS journal, 275 (2008) 4990-5006.

[42] N. Boy, J. Heringer, R. Brackmann, O. Bodamer, A. Seitz, S. Kölker, I. Harting, Extrastriatal changes in patients with late-onset glutaric aciduria type I highlight the risk of long-term neurotoxicity, Orphanet J. Rare Dis., 12 (2017) 77.

[43] K.P. Blemings, T.D. Crenshaw, R.W. Swick, N.J. Benevenga, Lysine-a-ketoglutarate reductase and saccharopine dehydrogenase are located only in the mitochondrial matrix in rat liver, JOURNAL OF NUTRITION-BALTIMORE AND SPRINGFIELD THEN BETHESDA-, 124 (1994) 1215-1215.

[44] S. Mihalik, W. Rhead, L-pipecolic acid oxidation in the rabbit and cynomolgus monkey. Evidence for differing organellar locations and cofactor requirements in each species, J. Biol. Chem., 264 (1989) 2509-2517.

[45] V.V. Rao, M.J. Tsai, X. Pan, Y.-F. Chang, L-pipecolic acid oxidation in rat: subcellular localization and developmental study, Biochimica et Biophysica Acta (BBA)-Protein Structure and Molecular Enzymology, 1164 (1993) 29-35.

[46] L. IJlst, I. de Kromme, W. Oostheim, R.J. Wanders, Molecular cloning and expression of human L-pipecolate oxidase, Biochem. Biophys. Res. Commun., 270 (2000) 1101-1105.

[47] V.V. Rao, Y.-F. Chang, Assay for l-pipecolate oxidase activity in human liver: detection of enzyme deficiency in hyperpipecolic acidaemia, Biochimica et Biophysica Acta (BBA)-Molecular Basis of Disease, 1139 (1992) 189-195.

[48] E. Okuno, M. Tsujimoto, M. Nakamura, R. Kido, 2-Aminoadipate-2-oxoglutarate aminotransferase isoenzymes in human liver: a plausible physiological role in lysine and tryptophan metabolism, Enzyme Protein, 47 (1992) 136-148.

[49] R. Posset, S. Opp, E.A. Struys, A. Völkl, H. Mohr, G.F. Hoffmann, S. Kölker, S.W. Sauer, J.G. Okun, Understanding cerebral L-lysine metabolism: the role of L-pipecolate metabolism in Gcdh-deficient mice as a model for glutaric aciduria type I, J. Inherit. Metab. Dis., 38 (2015) 265-272.

[50] I.A. Pena, L.A. Marques, Â.B. Laranjeira, J.A. Yunes, M.N. Eberlin, A. MacKenzie, P. Arruda, Mouse lysine catabolism to aminoadipate occurs primarily through the saccharopine pathway; implications for pyridoxine dependent epilepsy (PDE), Biochimica et Biophysica Acta (BBA)-Molecular Basis of Disease, 1863 (2017) 121-128.

[51] M. Hirashima, T. Hayakawa, M. Koike, Mammalian α-keto acid dehydrogenase complexes II. An improved procedure for the preparation of 2-oxoglutarate dehydrogenase complex from pig heart muscle, J. Biol. Chem., 242 (1967) 902-907.

[52] K. Majamaa, T.M. Turpeenniemi-Hujanen, P. Latipää, V. Günzler, H. Hanauske-Abel, I. Hassinen, K. Kivirikko, Differences between collagen hydroxylases and 2-oxoglutarate dehydrogenase in their inhibition by structural analogues of 2-oxoglutarate, Biochem. J., 229 (1985) 127-133.

[53] E.A. Sherman, K.A. Strauss, S. Tortorelli, M.J. Bennett, I. Knerr, D.H. Morton, E.G. Puffenberger, Genetic mapping of glutaric aciduria, type 3, to chromosome 7 and identification of mutations in c7orf10, The American Journal of Human Genetics, 83 (2008) 604-609.